Y/AMT-615

Y-12

OAK RIDGE
Y-12
PLANT

Final CRADA Report
for
CRADA Number Y-1296-0430

SENSOR DRIVEN INTELLIGENT CONTROL SYSTEM FOR PLASMA PROCESSING

RECEIVED
MAR 15 1999
OSTI

V. B. Campbell
Lockheed Martin Energy Systems, Inc.
Gary Bell
Lockheed Martin Energy Research
Gail Erten
Innovative Computing Technologies, Inc.

February 23, 1998

Approved for Public Release;
distribution is unlimited.

Prepared by the
Oak Ridge Y-12 Plant
managed by
LOCKHEED MARTIN ENERGY SYSTEMS, INC.
for the
U.S. DEPARTMENT OF ENERGY
under contract DE-AC05-84OR21400

MANAGED BY
LOCKHEED MARTIN ENERGY SYSTEMS, INC.
FOR THE UNITED STATES
DEPARTMENT OF ENERGY

UCN-13672 (2 11-97)

DISCLAIMER

This report was prepared as an account of work sponsored by an agency of the United States Government. Neither the United States Government nor any agency thereof, nor any of their employees, makes any warranty, express or implied, or assumes any legal liability or responsibility for the accuracy, completeness, or usefulness of any information, apparatus, product, or process disclosed, or represents that its use would not infringe privately owned rights. Reference herein to any specific commercial product, process, or service by trade name, trademark, manufacturer, or otherwise, does not necessarily constitute or imply its endorsement, recommendation, or favoring by the United States Government or any agency thereof. The views and opinions of authors expressed herein do not necessarily state or reflect those of the United States Government or any agency thereof.

DISCLAIMER

Portions of this document may be illegible in electronic image products. Images are produced from the best available original document.

ABSTRACT

This Cooperative Research and Development Agreement (CRADA) between Innovative Computing Technologies, Inc. (IC Tech) and Martin Marietta Energy Systems (MMES) was undertaken to contribute to improved process control for microelectronic device fabrication. Process data from an amorphous silicon thin film depostion experiment was acquired to validate the performance of an intelligent, adaptive, neurally-inspired control software module designed to provide closed loop control of plasma processing machines used in the microelectronics industry. Data acquisition software was written using LabView

The data was collected from an inductively coupled plasma (ICP) source, which was available for this project through LMES's RF/Microwave Technology Center. Experimental parameters measured were RF power, RF current and voltage on the antenna delivering power to the plasma, hydrogen and silane flow rate, chamber pressure, substrate temperature and H-alpha optical emission. Experimental results obtained were poly-crystallin silicon deposition rate, crytallinity, crystallographic orientation and electrical conductivity. Owing to experimental delays resulting from hardware failures, it was not possible to assemble a complete data for IC Tech use within the time and resource constraints of the CRADA. IC Tech was therefore not able to verify the performance of their existing models and control structures and validate model performance under this CRADA.

CRADA Objectives

- to use experimental data from a plasma etch process to validate the performance of process control software
- to validate the performance of process control software designed to optimize plasma processing of semiconductors used in the microelectronics industry using experimental data from a plasma etch process.
- measure (and make available to IC Tech) experimental parameters which will be incorporated into the process control module
- use the ORNL supplied process data to modify the appropriate model classes through neuro-fuzzy training
- validate IC Tech models using data collected from an inductively coupled plasma (ICP) source

The objectives above were not met owing to experimental delays resulting from hardware failures (damaged optical fiber, arc damage to RF voltage probe and vacuum pump failure). Small innovative companies developing new products require rapid turn-around in their product development and testing cycle. Experimental delays resulting from hardware failures, and deposited film analysis and characterization, coupled with limited project resources pushed the project beyond the time frame acceptable to IC Tech needs. The thin film results shown in the technical discussion resulted from a longer lived project which was executed in parallel to leverage resources. This leverage benifitted both projects in that the gas feed hardware and control systems were built up using support from the parallel project. CRADA resources were used to 1)design the experiment, 2)write the data acquisition software using LabView data acquisition hardware and programming and 3)assemble and install plasma light gathering optics, 4)install a fiber optic link between the plasma source and a Czerny-Turner spectrometer and 5)analyze spectral data to determine the dependence of SiH* emission intensity on process parameters. In addition, IC Tech was introduced to personnel at Texas Instruments working to develop neural based plasma process control algorithms.

The CRADA resulted in the instrumentation of an inductively coupled plasma source which contributed to the development of an advanced technique for the rapid deposition of poly-crystalline films. Data acquisition software was written, plasma light gathering optics were assembled and installed and a fiber optic link between the collection optics and a Czerny-Turner spectrometer was established and spectral data was acquired. These improvements in the diagnostic and data acquisition capabilities of the plasma source enhances the ability of Y-12 to win projects in the plasma chemical and physical vapor thin film deposition areas critical to the microelectronics industry. The project has already aided the lab in bringing in outside funding. The fact that Y-12 had devoted some internal money for applications of high density plasma sources for semiconductor processing helped to secure funding from SEMATECH and its member companies in excess of $4M for rf/plasma related research for CY 1996 and 1997. This interaction with SEMATECH is expected to grow and continue for some time. We have also made contacts at domestic flat panel display companies and supplier companies. Because of the similar physics and chemistry issues, we have submitted a white paper to DARPA on the use of high density plasmas for plasma metal organic chemical vapor deposition (MOCVD) for copper and high temperature superconductivity applications. The follow-on proposal will be for $1.2M per year for three years. In addition, the office of Energy Efficiency and Renewable Energy at DOE is being pursued for the superconducting wire research.

The primary DP benefit resides in its microelectronics mission:
i)improved capability of Y-12 to contribute to the improvement of radiofrequency (RF) systems used in etch and deposition systems. RF is seen by the semiconductor industry as key to the production of high reliability microelectronic devices.

ii)improved process control is critical to decreasing circuit feature size, which directly impacts performance (smaller, faster, more reliable). Defense electronics and advanced weapon system performance benefit directly.

iii)The data is available to developers of intelligent process control may lead to improved understanding of semiconductor processing and will contribute to reduced costs for integrated circuits as a result of improved yields.

ADVANCED DEPOSITION TECHNIQUES FOR PRODUCING THIN FILMS OF POLYCRYSTALLINE SILICON

John Caughman and Gary Bell/Fusion Energy Division
Dave Beach/Chemical and Analytical Sciences Division
Steve Gorbatkin/Solid State Division

BACKGROUND

A new technique has been demonstrated for depositing poly-crystalline silicon thin films for flat panel display applications. Thin films of poly-crystalline silicon (2000 Å) have been deposited in a way that will be compatible for use in thin film transistors, where substrate temperatures cannot exceed 500 °C. The technique combines a high density radio frequency (rf) inductively coupled plasma source with downstream gas injection that has resulted in device quality films deposited at rates that are higher than current state-of-the-art. Unlike conventional rf reactors, inductively coupled sources have high plasma and atomic species density along with low ion energies hitting the film surface during growth. The plasma chemistry can be better controlled by operating the source in a "downstream" mode, where the silane precursors needed for film growth are separated from the ionization region. For the growth of polysilicon thin films, this combination results in unique capabilities to control hydrogen stoichiometry, the relative rates of etching of poorly bound silicon, and to produce conditions favorable for the production of fine-grain polysilicon at temperatures >200 degrees lower than those used in conventional polysilicon chemical vapor deposition (650-700 °C).

EXPERIMENTAL SETUP

A schematic of the inductively coupled plasma source system that was used for the deposition is shown in Fig. 1. The source consists of a flat spiral coil that is separated from the vacuum region by a quartz window. The diameter of the chamber is 30 cm and the diameter of the coil is about 15 cm. Hydrogen gas is injected through a gas ring located near the plasma excitation region. A dense plasma is formed just under the window and acts as a supplier of atomic hydrogen to the process. Silane is injected through a gas ring located approximately 10 cm downstream from the source region. A heated substrate capable of handling 2 inch diameter samples is located approximately 10 cm downstream from the gas ring. High vacuum is maintained in the system by use of a turbomolecular pump that keeps the base pressure at 9×10^{-7} Torr. During deposition, the turbo pump is valved off and a high throughput roots pump system is used. Silane is transported from the gas bottle to the chamber through a vented gas cabinet and double walled tubing. Details of the gas handling system can be found in Appendix B.

The rf system consists of an L type matching network in series with the spiral coil antenna. An rf sensor used for measuring impedance and net power coupling was located between the coil and the matching network. The voltage and current couplers were calibrated previous to installation on the system. The impedance is composed of a real part and a reactive part. The real part corresponds to power deposition in the coil and in the plasma. The reactive part is dominated by the inductance of the coil. The magnitude of the rf impedance is given by the ratio of the voltage and the current. The resistive part of the load is found by dividing the input power by the square of the current. The reactive part of the load is then the square root of the difference between the square of the impedance magnitude and the square of the real part of the load.

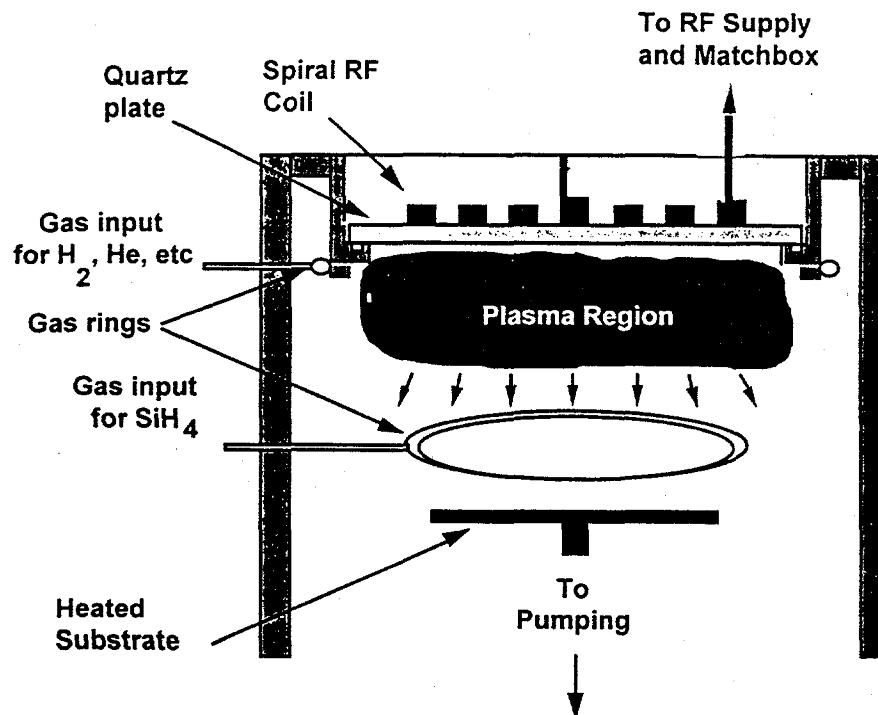

Fig. 1 Schematic of experimental setup. Hydrogen was injected near the source coil and the silane was injected downstream near the substrate.

The silicon was deposited on quartz substrates that measured either two inches in diameter or 1.4 inches square. The samples were clamped to the substrate holder and heated to the desired temperature. A small thermocouple was placed between one of the clamps and the sample to measure the temperature. After the sample reached the desired temperature, the turbo pump was valved off and the roots pump system was initiated. Hydrogen gas was injected into the system and the pump was throttled to achieve the desired pressure. A hydrogen plasma was typically run for approximately one to two minutes prior to silane injection for sample surface cleaning. No significant deposition was observed on the sample during this hydrogen cleaning phase. The temperature of the sample would typically rise 20-30 degrees during the hydrogen operation, and the voltage controlling the sample temperature would be decreased to maintain the desired deposition temperature. Deposition was initiated by injecting silane. After the deposition was

finished, the silane was turned off and the hydrogen plasma was run for an additional 10 seconds. The sample was then cooled until it reached a temperature below 200 C, the system was vented in nitrogen, and the sample was removed from the system (usually after it had reached a temperature below 100 C). Operating parameters that were varied included the pressure (15-1000 mTorr), rf power (100-1250 Watts), gas flows (H2:50-150 sccm, SiH4: 2.5-10 sccm), sample temperature (100-400 C), and deposition times (2-16 minutes).

Techniques used for evaluating the films after deposition included Raman Spectroscopy, X-Ray diffraction, film thickness (measured with a surface profilometer), and electrical conductivity. The Raman system used a 514.5 nm argon laser, a 40x objective lens, 4 x 400 micron slits, a step size of 0.25 wavenumbers, and an integration time of 1 sec/step. Unless noted otherwise, all scans shown are an average of 4 consecutive scans over the indicated range. The laser power at the samples was about 30 mW. The X-ray diffractometer used a CuKα radiation source with a wavelength of 1.5406 Å.

EXPERIMENTAL RESULTS

A. RF Power Coupling

The impedance of the coil can give insight into the type of power coupling taking place. With inductively coupled plasma sources, there is always some level of capacitive coupling. Capacitively coupled discharges typically have low plasma densities, high rf voltages in the plasma, and high ion energies bombarding the substrate. Inductively coupled plasmas typically have high plasma densities, lower rf voltages in the plasma, and low ion energies at the substrate. The load resistance as a function of input power is shown in Fig. 2 for a hydrogen plasma at 50 mTorr and 200 mTorr. The flow of hydrogen was 150 sccm for both pressures. The transition from the capacitively coupled mode to the inductively coupled mode can be seen by observing the change in the real part of the coil impedance as a function of input power. The capacitive mode has low plasma loading, which means that more power is dissipated in the rf losses in the coil and less power is coupled into the plasma. As the input power increases, the loading gets better and reaches a steady level as the discharge becomes dominated by inductive coupling. The transition power range is dependent on the gas species and the gas pressure. For the 50 mTorr condition, the loading has started to level off after reaching an input power of 1000W, while the loading is still increasing for the 200 mTorr condition as the power reaches 1300 W. The significance of this coupling mode is that the plasma density and the amount of atomic hydrogen production increase as more power gets coupled inductively. We observed that deposition rates increased with rf power as we moved from a loading area that was dominated by capacitive coupling to an area that was dominated by inductive coupling.

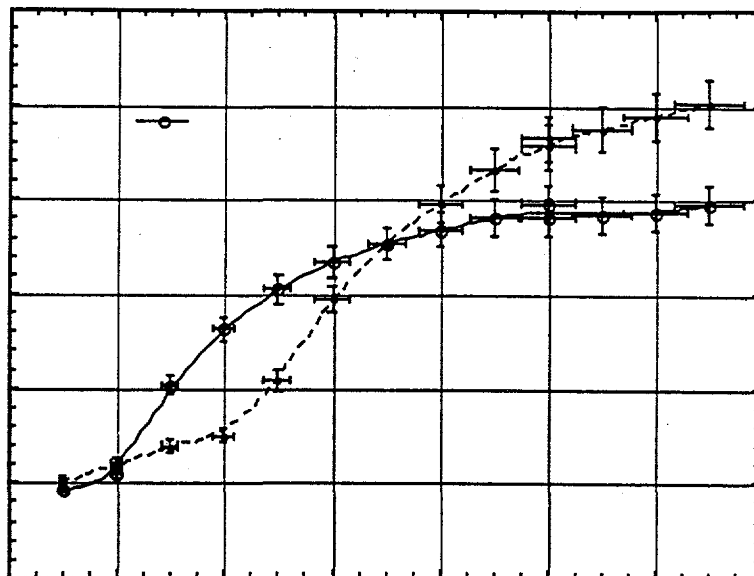

Fig. 2 The antenna load resistance as a function of input power for a 50 mTorr and a 200 mTorr plasma. The transition from capacitive mode to inductive mode can be seen as the load impedance increases with power.

B. Film Thickness

The thickness of the films was measured over a wide range of operating conditions. An example of some of the data is shown in Table I. The deposition rate was calculated by dividing the film thickness by the deposition time. The deposition rate increased as the pressure was dropped from 200 to 50 mTorr, while the flow rates remained the same. The decrease in pressure was obtained by increasing the pumping speed by opening the throttle valve on the pump. This increase in gas flow through the reactor has the effect of decreasing the residence of the reactants in both the ionization zone and the reaction zone as well as increasing the mean free path and decreasing the collision frequency. It was also observed that the deposition rate has only a weak dependence on silane flow rate. A decrease in the silane flow rate from 10 to 2.5 sccm caused a minor decrease in the deposition rate. The deposition rate is fairly steady with time, as indicated in Fig. 3. These data are for a pressure of 50 mTorr, a hydrogen flow of 150 sccm, a silane flow of 10 sccm, a temperature of 370 °C, and an rf power of 1000W.

Pressure (mTorr)	H2 flow (sccm)	SiH4 flow (sccm)	RF Power (W)	Dep rate (nm/min)
200	100	10	1000	27
50	100	10	1000	80
50	50	10	1000	75

50	150	10	1000	60
50	150	5	1000	58
50	150	2.5	1000	46
50	150	5	1250	45

Table I. An example of deposition rate as a function of processing parameters.

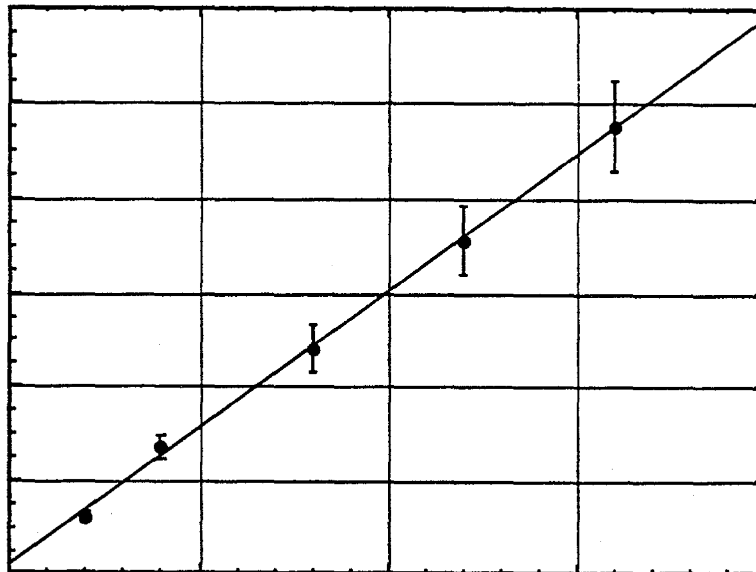

Fig. 3 The variation of film thickness as a function of deposition time. The deposition rate appears to be linear with time.

C. Crystallinity

The crystallinity was determined by analyzing and deconvolving the Raman spectrum. All the films deposited showed a fairly high volume fraction of polycrystalline structure. A typical spectrum is shown in Fig. 4. The conditions for this example are for a pressure of 50 mTorr, a hydrogen gas flow of 150 sccm, a silane gas flow of 3 sccm, a temperature of 370 °C, and an rf power of 1000W. For a pure crystalline sample, the Raman peak is at 520 wavenumbers. Our data consistently show a down-shift in this peak to around 514 cm^{-1}, which may be due to film stress or impurities.[1] However, based on the low conductivity results to be discussed later, a high level of impurities in the film seems unlikely. A best fit to the data is for a 3 Gaussian fit, with crystalline peaks at 514 and 503 cm^{-1} and an amorphous peak at 480 cm^{-1}.[1] This choice is consistent with having a crystalline component near the 520 cm^{-1} peak and a collection of small crystallites contributing to the peak near 500 cm^{-1}.[2] The semiquantitative crystalline volume

fraction can be determined as Xc = Ic / (Ic + Ia), where Ic is the integrated intensity of the crystalline peaks (514 and 503 cm^{-1}) and Ia is the integrated intensity of the amorphous peak. The width of the spectra will also decrease as the crystalline fraction increases. For the spectra shown in Fig. 4, the crystalline volume fraction is about 80% and the full-width-half-max (FWHM) is 12.3. For fixed pressure, there was a weak dependence observed on the position of the peak of the spectrum and the degree of crystallinity of the films as a function of gas flow ratio, based on the Raman data for those samples. Lower silane flows gave roughly the same cystallinity as higher silane flows, but for thinner films.

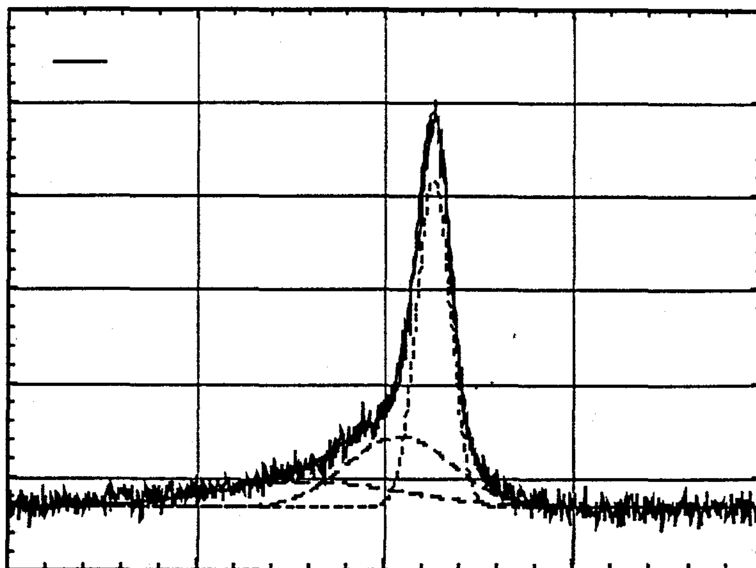

Fig. 4 An example Raman spectrum where the best fit to the data is for three Gaussian peaks. The crystalline peaks are for wavenumbers of 514 and 503 cm-1, and the amorphous peak is at 480 cm-1.

There was a shift in the peak and the degree of crystallinity as a function of deposition time (or film thickness) for fixed processing conditions, as shown in Fig. 5. The processing conditions were for a pressure of 50 mTorr, a hydrogen flow of 150 sccm, a silane flow of 10 sccm, a temperature of 360 °C, and an rf power of 1000W. As the film gets thicker, the peak in the spectrum shifts from 507 cm^{-1} for a thickness of 270 nm (4 min) to around 515 cm^{-1} for a thickness of 710 nm (12 min). As the film continues to grow, the peak shifts down to around 513 cm^{-1} at a thickness of 950 nm (16 min), which seems to be due to an increase in the contribution from the Gaussian centered near 500 cm^{-1}. The FWHM also decreases as the film gets thicker and reaches a steady-state value of 11 after a thickness of 710 nm is reached. The degree of crystallinity also appears to increase with film thickness and also seems to reach a steady-state value after a thickness

of 710 nm. As the film grows, the structure changes from an amorphous/crystalline mix to a film that is dominated by a crystalline structure. As will be shown in the next section, this structure is due to a preferred orientation of the grains as the film grows.

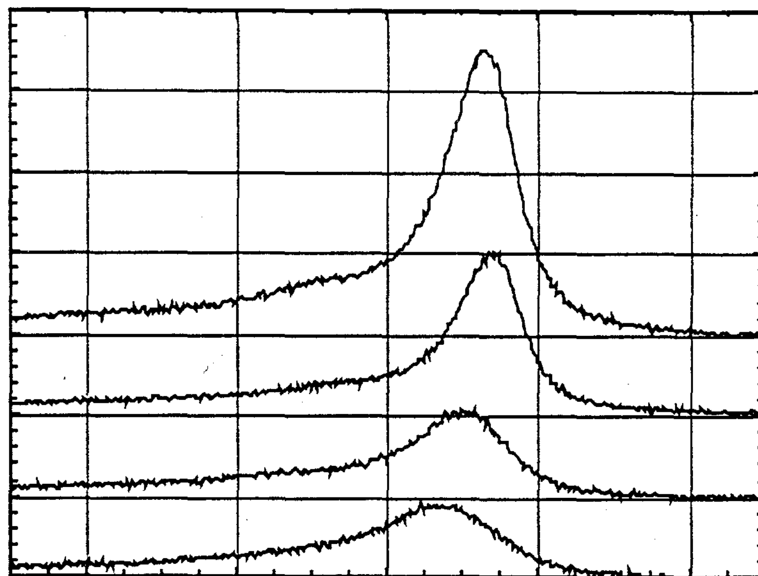

Fig. 5 The Raman spectrum evolves as the film gets thicker. The peak in the spectrum shifts to higher wavenumber and the film gets more crystalline as it grows until a steady-state condition is met. The growth of the film is nearly linear in time, with the thickness increasing from about 270 nm to about 950 nm for a deposition time from 4 min to 16 min (see Fig. 3)

D. Crystallographic Orientation

Information on the orientation of the films can be found by looking at the X-ray diffraction intensity. An example x-ray diffractogram is shown in Fig. 6. The conditions for this sample were for a pressure of 50 mTorr, a hydrogen gas flow of 100 sccm, a silane gas flow of 10 sccm, a temperature of 360 °C, and an rf power of 1000 W. The thickness of this film was 800 nm. The broad peak near an angle of 22 is due to the quartz substrate on which the film was grown. Also shown in the figure are relative peak heights for a silicon sample with randomly oriented crystalline structure. There is some contribution from the (111) peak and weak signal from the (311) peak.

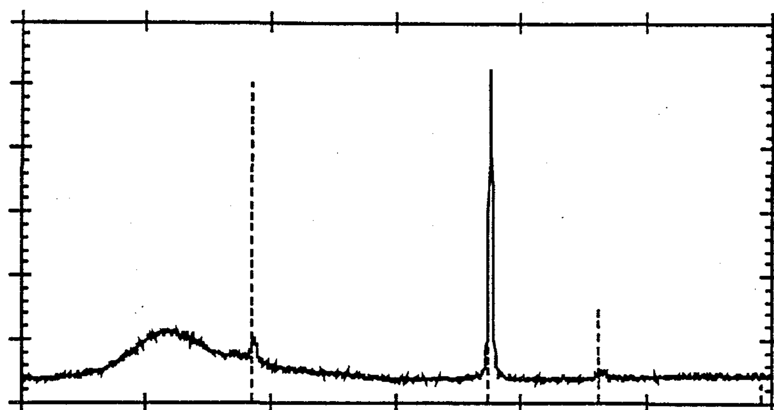

Fig. 6 X-ray diffractogram of a polysilicon film deposited on quartz. The broad peak at 22 is due to the substrate and the dotted lines correspond to the relative peak intensities for a randomly oriented silicon sample.

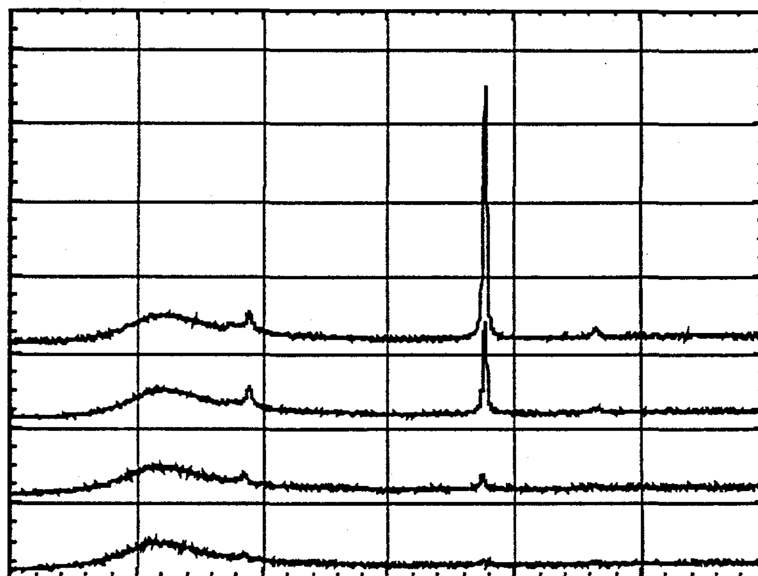

Fig. 7 The preference for the <110> crystalline orientation, corresponding to the (220) peak in the X-ray diffractogram, increases as the film thickness increases.

As with most of the deposition results, there is a strong preference for the 220 peak, which corresponds to the <110> crystal orientation. This preference exists for a wide range of operating conditions. At an operating pressure of 200 mTorr, the (220) peak is

slightly higher than that of a sample of similar thickness run at 50 mTorr, although the deposition rate is higher for the 50 mTorr condition.

The preference for the (220) peak increases with film thickness. A plot of the X-ray diffraction intensity as a function of film thickness (deposition time) is shown in Fig. 7. The conditions for this set of data were the same as for the Raman spectra results shown in Fig. 5. The intensity of the (220) peak increases faster than the film thickness, although the film thickness increases close to linearly with time. The deposition rate does not change appreciably with time, even though the preference for the <110> orientation becomes more dominate as the film gets thicker.

E. Conductivity

The conductivity of the samples were determined by measuring the current and voltage across a set of electrodes deposited on the surface of the samples. One inch long aluminum strips with a width of 1 mm, a thickness of 150 nm, and a spacing of 1 mm apart were evaporated through a shadow mask onto the surface of the films. A voltage was placed across adjacent electrodes and the current was measured to give total resistance, R_{total}. The voltage was adjusted to insure that measurements were made in the linear voltage/current regime. The conductivity of the film was then determined by dividing the spacing between the electrodes (0.1 cm) by the product of the measured resistance (R_{total}), the length of the strip (2.54 cm), and the thickness of the film. Conductivities were fairly low and ranged from 1.7×10^{-7} S/cm to 8.5×10^{-6} S/cm. The best (lowest) conductivity measured was for a pressure of 50 mTorr, a hydrogen flow of 150 sccm, a silane flow of 5 sccm, a temperature of 390 °C, and an rf power of 1250 W, while the worst conductivity measured was for the same conditions but with a temperature of 135 °C. This low conductivity implies that the impurity content in the films was not very high. Oxygen incorporation in polysilicon films has been shown to increase the conductivity.[3] Based on the low conductivities measured for our films, however, the oxygen content was probably low.

DISCUSSION

During film growth, the flux of hydrogen and silane species at the substrate results in a combination of deposition and etching processes. The flux of atomic hydrogen etches elements of the film during deposition. Atomic hydrogen preferentially etches weaker amorphous bonds relative to crystalline bonds. The high degree of crystallinity shown in the Raman and the X-ray diffraction data is consistent with the presence of a high flux of atomic hydrogen bombarding the surface during film growth. The degree of crystallinity increases as the film increases. As the film gets thicker, there is a large preference for the <110> orientation. This preference has been explained in terms of a combination of preferred nucleation and etching.[2] The nucleation of the <111> orientation requires three bond sites, while the <110> orientation requires two. Therefore, it is easier to nucleate the <110> orientation, while the etching of these two orientations is similar. Nucleation of the <100> is preferred even more, but the etching of this orientation is even faster. The results shown in the X-ray diffraction data is similar to that seen with plasmas

containing large amounts of SiF_4.[2,4] The fluorine strongly etches the silicon in a way similar to the hydrogen. We have been able to achieve similar results using just hydrogen, which eliminates the possibility of F incorporation in the films.

We have shown that an inductively coupled plasma source is ideal for depositing high quality thin films of polysilicon at low temperatures. The processing conditions favorable for polysilicon growth have been discovered by analysis of the power coupling mechanisms for plasma enhanced chemical vapor deposition (inductive vs capacitive coupling). Our deposition rates (up to 80 nm/min) are greater than those previously published in the literature (<12 nm/min). The conductivity of the films is quite good (10^{-7} S/cm), and the crystallinity is excellent (>80%). We have been able to deposit films at a preferred grain orientation due to the etching of poorly bound silicon by the presence of large quantities for atomic hydrogen at the surface during film growth. This preferred orientation deposition has applications outside of polysilicon, including high temperature superconducting wire. Orientation of the buffer layer and the superconducting film may be possible. Another potential application are is in the deposition of copper for microelectronics. It has been shown in the literature that deposition rates of copper deposited by CVD increase with the presence of atomic hydrogen. Our method is one that is transferable to manufacturing and is compatible with large area deposition for use in flat panel display, microelectronics, and superconducting wire applications.

REFERENCES

1. M. Luysverg, P. Hapke, R. Carius, and F. Finger, "Stucture and growth of hydrogenated microcrystalline silicon: investigation by transmission electron microscopy and Raman spectroscopy of films grown at different plasma excitation frequencies", Philosophical Magazine A, 1997, Vol. 75, No. 1, pp. 31-47.

2. H. Kakinuma, M. Mohri, M. Sakamoto, and T. Tsuruoka, "Structural properites of polycrystalline silicon films prepared at low temperature by plasma chemical vapor deposition", J. Appl. Phys. 70 (12), 15 December 1991, pp. 7374-7381.

3. P. Torres, et al., "Device grade microcrystalline silicon owing to reduced oxygen contamination", Appl. Phys. Lett. 69, 1373 (1996).

4. K.-Y. Choi, C.W. Lee, and C. Lee, "Substrate-Dependent growth of polycrystalline silicon films prepared by plasma-enhanced chemical vapor deposition using SiF4 and H2 gases", Jpn. J. Appl. Phys., Vol. 34 (1995), pp. 4673-4676.

Appendix A: Silane gas handling system

Primary Reference: "Evaluating Risks Associated with the Use of Silane", P. D. Moskowitz, V. M. Fthenakis, R. W. Youngblood, and S. R. Mendez, in Hazard Assessment and Control Technology in Semiconductor Manufacturing, American Conference of Governmental Industrial Hygienists, Lewis Publishers, 1987.

The principal hazard associated with the use of silane is that it is spontaneously flammable under some conditions. Mixtures of silane and air below 2% silane (0.5% with hydrogen present) will not spontaneously ignite. Higher concentrations of silane in air can also be formed which do not spontaneously inflame, but rather detonate, which means creation of a shock wave and over pressure. However, the use of good ventilation and appropriate controls will allow for safe operations. Engineering controls include all of the following: 1) Limitation of the amount of silane to less than 100 grams, 2) Limitation of cylinder pressures less than 150 psig, 3) Use of flow restricting devices, 4) Use of gas cabinets and double-walled ventilated tubing, 5) Use of all-welded stainless steel regulators, cross-purging manifold, and tubing capable of withstanding pressures in excess of 600 psig, 6) Dilution of silane to concentrations below those known to detonate using inert gas, and 7) Use of appropriate interlocks and pressure sensing devices to detect failure of any critical component in the system such as vacuum pumps, exhaust gas ventilation and inert-gas dilution. The system is depicted in Figure A1.

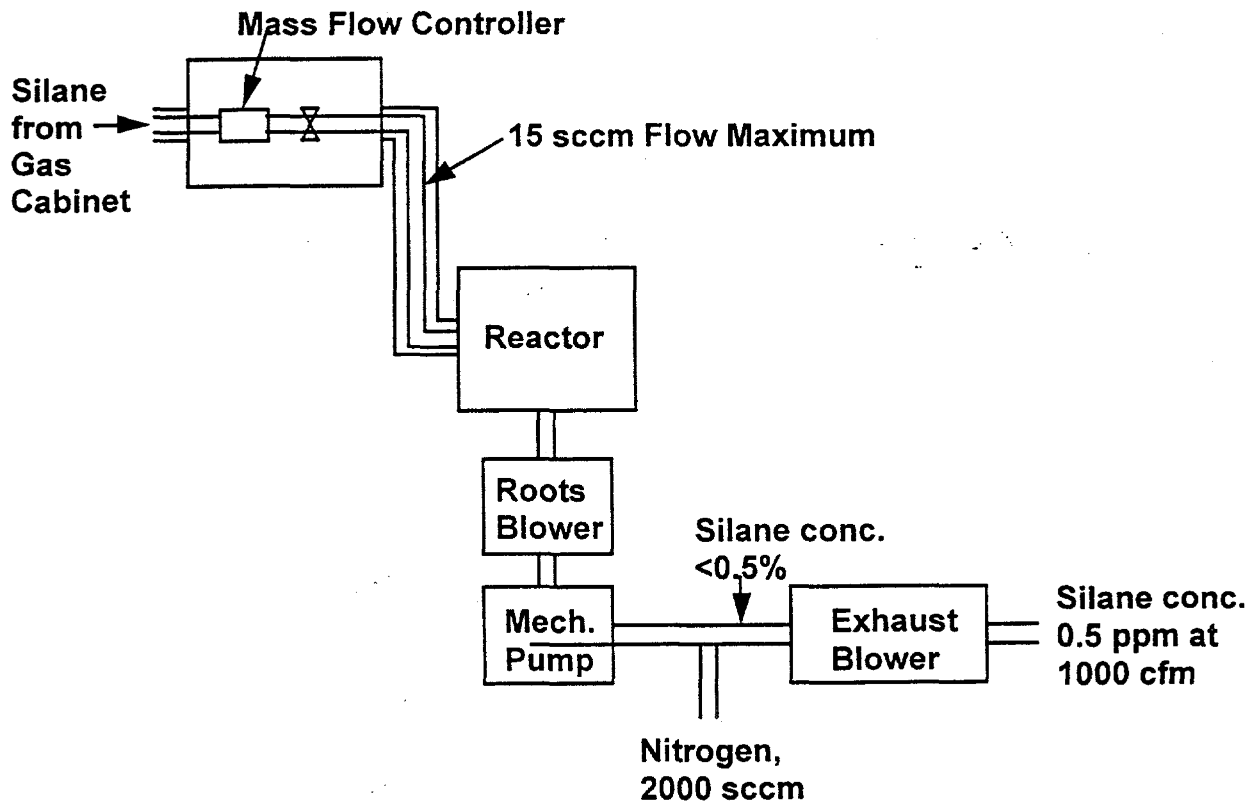

Figure A1. Gas handling system

Gas Cabinet

A typical silane gas cabinet is depicted schematically in Figure A2. The metal gas cabinet is located inside a vented hood. A flow indicator is connected to the exhaust of the hood to sense that the vent system is operating. This flow indicator is part of the interlock system to allow for safe operations. From the cylinder, a flow restrictor, 6 mil in diameter, is installed in the CGA fitting attached to the cylinder. This will limit flow to 2 liters/min so that it would require 35 minutes for the entire cylinder volume to be vented. With adequate cabinet ventilation (25 cfm, 520 l/min), no explosive detonation would occur because mixtures of silane and air below 2% (0.5% with hydrogen present) do not ignite. There would be some risk of fire within the cabinet in the immediate vicinity of the leak. However, with silane flowing at only 2 liters/min, the damage would be minimal and confined to the cabinet. The cross-purge is used in the event of regulator or pneumatic valve failure to remove silane trapped within the volume of the manifold. While the cross-purge could be used to purge the regulator after silane cylinder changes, this will typically not be necessary because the manifold may be evacuated and leak tested using the reactor vacuum. A single-stage regulator will lower the pressure to 5 psig, the required inlet pressure for the mass flow controller. A pneumatic valve is used to shut-off silane flow in the event of any of the following: 1) Loss of cabinet exhaust or system exhaust, 2) Reactor pressure above 10 torr (pump failure) 3) Loss of flow in the nitrogen purge line. A plastic tube is used between the pneumatic valve and the electrical solenoid so that the unlikely event of a fire in the cabinet would cause the tube to melt which causes the valve to close and the flow of silane to cease.

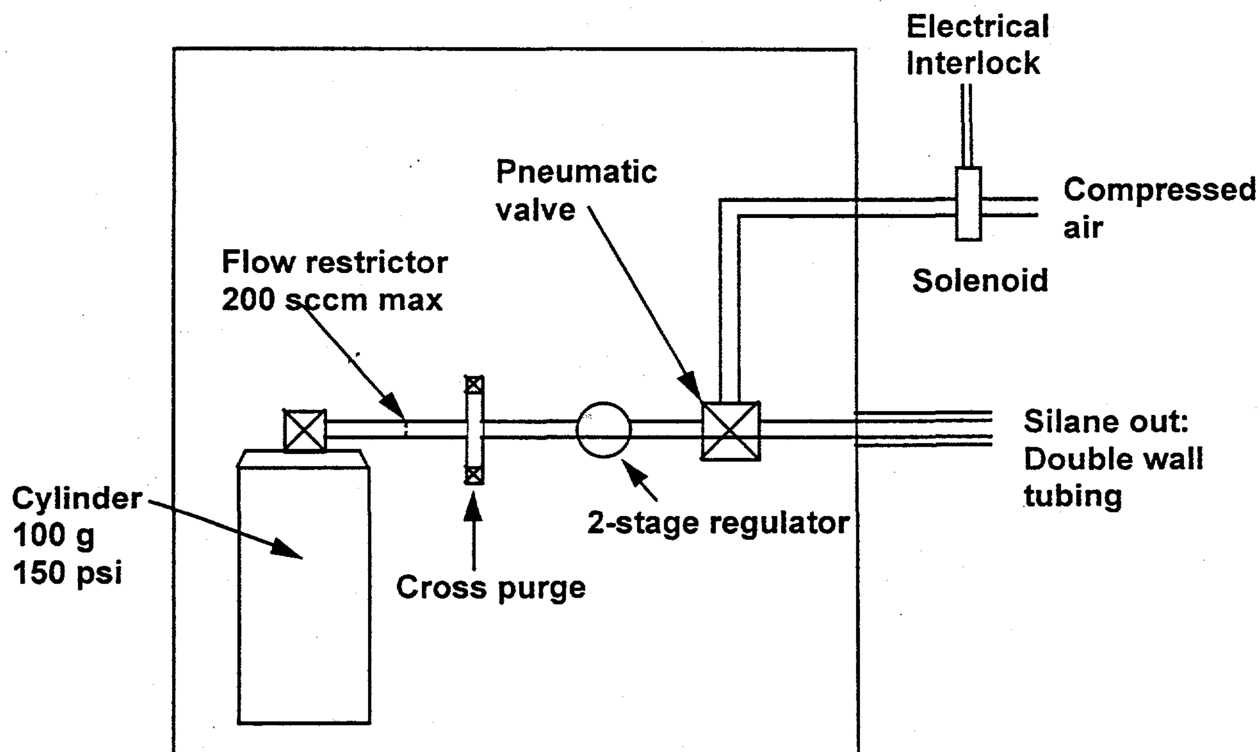

Figure A2. Gas cabinet detail.

Flow Controller Box

From the gas cabinet, silane will flow through a welded 1/4" stainless steel line to the flow controller box. The line is jacketed with 1-1/2" S.S. tubing and is exhausted through the gas cabinet. The flow controller box is also exhausted through the gas cabinet. The flow controllers contained in the box have air operated-normally closed valves to prevent silane leak-through. These valves are also controlled by the interlock system used to control the gas cabinet air valve. The flow controller is a MKS 10 sccm unit which also serves as another level of flow restriction since the size of the flow valve limits total flow to less than 150% of the flow meter rating (15 sccm max) at 150 psi of inlet pressure.

Reactor

Flow of silane in the reactor is through a gas dispersion ring slightly downstream of the plasma. Most of the silane will be consumed in normal operation. Pressure in the reactor will be monitored using capacitance manometer gauges. Excessive (more than 10 torr) reactor pressures are sensed by a pressure switch (set at less than 10 Torr) and the flow of silane will be halted. There is no ignition source/oxidizer in the reactor. In the case of an air leak, the pressure valve will trip the interlock system and the flow of silane will stop.

Pumps

The pumps used in the system are 1) two-stage Roots-blower which has a hermetically sealed motor and uses non-flammable Krytox fluorocarbon lubricant, and 2) a Leybold-Heraeus two-stage mechanical pump also using Krytox fluid.

Exhaust System

Exhaust gases from the mechanical pump is immediately mixed with nitrogen flowing at a minimum rate of 2 liters/min. This will result in a maximum silane concentration of 0.5% at the maximum silane flow rate of 10 sccm, thus rendering the mixture not spontaneously flammable. Flow of purge gas is part of the interlock system and is monitored using a mass-flow meter.

Interlock System

The interlock system is composed of a flow indicator on the gas cabinet/hood vent, a pressure switch on the reactor chamber, and a flow controller on the pump exhaust purge system. The interlocks are connected to a 24 Vdc solenoid that controls the air supply for the pneumatic valves that control the flow of silane in the system. For the pneumatic valves to open and allow for the flow of silane, all of the following conditions must me met: 1) hood exhaust must be on, 2) pressure in the reactor chamber must be less than 10 Torr, and 3) the nitrogen purge line on the pump exhaust must have a flow of at least 2 liters/min.

Inventions

No inventions were made or reported.

Assessment of commercialization possibilities

Commercialization is uncertain at this time. Individual companies in the microelectronics production industry are known to be working on neural-inspired control algorithms. IC Tech may or may not revisit this business opportunity depending on market forces and the availability of research and development funding.

Plans for future collaboration

We have no firm plans for future collaboration at this time. ORNL remains available to make introductions and facilitate research and development efforts in the process control and microelectronics fabrication industries.

CONCLUSIONS

The objects of the CRADA were partially met. CRADA resources were leveraged with resources from a parallel project to the benefit of both efforts. Using CRADA funds, an inductively coupled plasma source was instrumented with RF current and voltage detectors and coupled via focusing optics and an optical fiber to a Czerny-Turner spectrometer. LabView based data acquisition software was written and used to collect process data. Owing to hardware failures and film characterization delays, the experimental plan was not completed within the time and resource contraints of the CRADA. IC Tech did not obtain the process data which was to be used to validate their control software. IC Tech requires rapid turn-around in its product development cycle and the experimental delays encountered pushed project completion beyond the time when the data could have been utilized to fulfill IC Tech's planned contribution to the CRADA. The available CRADA resources were not sufficient to overcome the hardware failures. The data presented in the body of the report were achievable owing to the leveraged effort. IC Tech contributed equally to the project planning.

Distribution:

Bruce Campbell, MS-8095, 9202
Gary Bell, MS-8071 9201-2
Chris Valentine, MS-8242, 701SCA
Ray Ford, MS-8084, 9203 (RC)
DOE/ORO, FOB, Room G-209
Joyce Shepherd, MS-6416 5002
P. L. Gorman, MS-6269, 4500-N
Laboratory Records, MS-6285, 4500-N
Y-12 Central Files, MS-8169, 9711-5

Gail Erten, Innovative Computing Technologies, Inc., 2157 University Park Dr., Okemos, MI 48864 (5 copies)